DUAL-WAVELENGTH OF 1.3μm AND 1.55μm AlGaSb/GaSb ASYMMETRIC QUANTUM-WELL LASER

Steven K. H. Sim[a], Kabula Mutamba[b], and E. Herbert Li[c]

Department of Electrical and Electronic Engineering, University of Hong Kong,
Pokfulam Road, Pokfulam, Hong Kong.
[a]k.sim@ieee.org
[c]ehli@eee.hku.hk
Institut für Hochfrequenztechnik, Technische Universität Darmstadt,
Merckstraße 25, 64283, Darmstadt, Germany.
[b]di1h@hrzpub.tu-darmstadt.de

Abstract

A dual-wavelength laser diode of 1.3μm and 1.55μm operating wavelength is under analysis. The structure of this laser diode involves an asymmetric dual quantum-well of $AlGaSb/GaSb$. The longer-wavelength quantum-well is doped with a 50Å Si at the barrier near the well. This will enable a localized intermixing during an anneal under a SiN_x cap, while the shorter-wavelength quantum-well is not affected. The area where $GaSb$ is exposed has no intermixing in both the quantum-wells. It is possible to construct a dual wavelength quantum-well laser where the surface is pattered to have a section covered with SiN_x and the other has $GaSb$ exposed. The $GaSb$-exposed section undertakes surface lasing at 1.55μm, while the SiN_x capped section removes the longer wavelength quantum well by intermixing and lasing at 1.3μm.

1. Introduction

Small band-gap material Antimonide(Sb) has been one of the focus of researches because of its potential for both high-speed and long-wavelength optical devices. Researches specifically are interested in its band-gap properities. When Sb combines with aluminum(Al) to form $AlSb$ alloy, its band-gap energy is around 2.3eV, giving a relative high potential barriers for quantum-well structure, hence providing better quantum confinement. While Sb combines with Indium(In) and Asenide(As) to form $InAs_xSb_{1-x}$ at x=0.4, its band-gap will reduce to around 0.01eV. Which is the smallest band-gap available by any III-V seminconductor alloy. This small band-gap material properities enable detection or emission of wavelength as long as 14μm using the interband transition. This material is also good for quantum-well structure because it is easy to find another alloy to form either strained or un-strained quantum-well sturcture for different device applications.

Semiconductor laser diode of mutliple wavelength emission are of interest to many applications, such as laser color printing, wavelength division multiplexing in optical communication system and

multiple wavelength optical recording. It is very important for such laser diode device to be fabricated in a way that the two emission wavelengths can be integrated close together physically while maintaining a wide spectral separation. In an multiple wavelength optical system, it is necessary to use a complicated lens system for the focus of each discrete emitter, while an emitter with source that is physically close together can save up all those complicated lens focusing systems. Researches around the world have proposed several designs which involve the entire laser structure grown on top of another one, where terraces are then etched to contact the various devices[1-3]. However, the result is a highly non planner structure, where the two emitting spots are more than 2μm apart in the growth direction, the separation increases when more than two wavelengths are integrated. Some other designs involve the combination of etching and selective area growth[4-6]. In this design, each additional wavelength integrated requires a separate growth of another layer. There is another technique introduced by Beernink et. al.[7], where single regrowth after patterned etching is required for multiple wavelengths. In this presentation, we will report a dual-stripe dual-wavelength[8] laser diode with antimonide based material and emission wavelengths of 1.3μm and 1.55μm. This technique has an advantage over other designs that it does not involve any layer regrowth and uses selective area intermixing technique for wavelength tunning.

2. Theoretical Model of Diffused Quantum-Well

The quantum-well structure modeled in this paper is $Al_xGa_{1-x}Sb/GaSb$ single quantum-well. Although the device sturcture is an asymmetric quantum-well, the width of the barrier between the two quantum-well is relatively thick. We can model each quantum-well alone, and diffusion will only occur at the well that have a thin layer of grown-in Si.

The Al composition profile, $\widetilde{w}(z)$, across the quantum-well structure is given by[9]

$$\widetilde{w}(z) = w_0\left\{1-\frac{1}{2}\left[erf\left(\frac{L_z+2z}{4L_d}\right)+erf\left(\frac{L_z-2z}{4L_d}\right)\right]\right\}, \tag{1}$$

where w_0 is the as-grown Al mole fraction in the barrier, L_z is the as-grown width of the quantum-well, z is both the quantization, the growth axis and $erf(\ )$ is error function[10] and L_d is diffusion length, which is defined as $L_d = (D\times t)^{\frac{1}{2}}$, where D and t are the diffusion coefficient and the annealing time, respectively.

Equation (1) is utilized to obtain the band-gap energy $\widetilde{E}_g$, the well-barrier discontinuity $\Delta\widetilde{E}_g$, and the well depth $\Delta\widetilde{E}_r$, and is defined as follows:

$$\widetilde{E}_g(z) = E_g(w=\widetilde{w}(z)),\quad \Delta\widetilde{E}_g = E_g(w_0)-\widetilde{E}_g(z=0),\quad \Delta\widetilde{E}_r = Q_r\times\Delta\widetilde{E}_g,$$

where the subscript r denotes either the electron in the conduction band (C), heavy or light holes

in the valance band (V=H or L). The interdiffusion-induced quantum well confinement profile $U_r(z)$ is defined as

$$U_r(z)=Q_r\left[\widetilde{E}_g(z)-\widetilde{E}_g(z=0)\right]. \tag{2}$$

We have defined the zero potential to be at the bottom of the interdiffused quantum-well and positively up in both bands except for valence subband mixing, which is taken to be negative down; the absolute position of this zerp potertial varies with L_d and the band offset splitting Q_r.

The valence subband structure is described by a multiband effective-mass approximation based on the $k \bullet p$ method of Lüttinger and Kohn[11]. By using Ben-Daniel and Duke model[12], the electron and holes at the zone center of Γ_6-valley symmetry can be calculated separately, with a z-position dependent effective mass on the interdiffused composition profile. The one-dimensional Schrödinger-like equation, for the envelope function $\Psi_{rl}(z)$, is then written aas follows:

$$-\frac{\hbar^2}{2}\frac{d}{dz}\left[\frac{1}{m^*_{\perp r}(z)}\frac{d\Psi_{rl}(z)}{dz}\right]+U_r(z)\Psi_{rl}(z)=E_{rl}\Psi_{rl}(z) \tag{3}$$

where $l=1,2,\ldots$ are the quantum-well subband levels for either the electrons (Cl) or holes (Vl), respectively; $m^*_{\perp r}(\widetilde{w}(z))$ is the carrier effective mass in the z direction; $E_{rl}\equiv E_{rl}(k_{//}=0)$ is the subband-edge energy, and the origin of the potential energy is taken at the bottom of the error function profile quantum-well. The above equation is solved numerically using finite difference method with the confinement profile defined in equation (2) and the boundary conditions are taken to be zero at the end of the finite and large barrier $\left[\Psi_{rl}(\pm z_f)=0\right]$; in other words, the error function profile quantum-well is embedded in a well of width $L_f=2z_f$ with an infinitely high barrier to approximate the thick barrier.

As for finite $k_{//}\neq 0$, the electron non-parabolic in-plane dispersion can be modeled by a fourth-order expansion with the coefficients $(\alpha_0 and \beta_0)$ determined using a 14 band $k \bullet p$ calculation[13]. Neglecting the spin-orbit splitting term and keeping only an anisotropic fourth-order term, the dispersion energy can be expressed as

$$E_C(k)=\alpha_0 k_z^4+\frac{\hbar^2}{2m_c^*}\left(k_z^2+k_{//}^2\right)+\left(2\alpha_0+\beta_0\right)k_z^2 k_{//}^2. \tag{4}$$

It is more difficult to solve the valence subband dispersion since coupling mixes the heavy and light hole states for $k_{//}\neq 0$, thus preventing the diagonalization of the fourfold-dgenerated Lüttinger Hamiltonian which can be solved using an effective hamiltonian developed by Chan.[14] The effective Hamiltonian is

$$\begin{bmatrix} E_{3/2} & C & B & 0 \\ C^* & E_{-1/2} & 0 & B^T \\ B^* & 0 & E_{1/2} & C^T \\ 0 & B^* & C^* & E_{-3/2} \end{bmatrix}, \tag{5}$$

where

$$C_{ll'} = \left[\frac{3}{4}\right]^{\frac{1}{2}} \frac{\hbar^2}{m_0}\gamma_2\left(k_x - ik_y\right)^2 \int_0^{L_f} dz \Psi_{-3/2,l}(z)\Psi_{1/2,l'}(z), \tag{6}$$

$$B_{ll'} = 3^{\frac{1}{2}} \frac{\hbar^2}{m_0}\gamma_2\left(-k_x - ik_y\right)\int_0^{L_f} dz \Psi_{3/2,l}(z)\frac{\partial}{\partial z}\Psi_{-1/2,l'}, \tag{7}$$

$$E_{\pm 3/2,ss'} = \delta_{ss'}E_{Hs} - \frac{\hbar^2}{2m_{//H}}k_{//}^2, \tag{8}$$

$$E_{\pm 1/2,ss'} = \delta_{ss'}E_{Ls} - \frac{\hbar^2}{2m_{//L}}k_{//}^2, \tag{9}$$

$\gamma_2(w)$ is the Luttinger parameter, and L_f is the width of a square quantum-well with infinitely high barriers which contains the error function profile quantum-well.

3. Results and Disscussions

In this presentation, we have modeled two dual-stripe dual-wavelength laser diodes. Both of the design do not involve any re-growth at the active region. The difference between the two design is that one makes use of localized intermixing to adjust the quantum well until its interband transistion emits the wavelength of 1.3μm, while the other one also makes use of localized intermixing, but to remove the quantum-well that will emit 1.55μm wavelength completely. Figure 1 shows the simplified schematic band diagram for the active region of the two designs.

Since the barriers between any of the two quantum-well is relatively thick, we model each quantum-well separately. The first design models a single quantum-well of 82Å well width $Al_{0.35}Ga_{0.65}Sb/GaSb$, with a 50Å thin layer of grown-in Si and is utilized to increase the $Al-Ga$ interdiffusion coefficient in the region. This as-grown quantum-well has a transition energy of 800meV which gives out light at 1.55μm wavelength. A SiN_x is capped on the surface of the sample and a stripe of SiN_x cap is cut open. The structure is then annealled for a calculated time, where an intermixing of Al and Ga atoms occurs locally on the side where the SiN_x cap is on. The diffusion ceases until the transition energy of the quantum-well is 952meV, giving out a 1.3μm wavelength in our case, we have calculated the diffusion length to be 36Å. Now we have a structure that gives out light at 1.55μm(uncapped) and 1.3μm (SiN_x capped)

The second design models two single quantum-wells of 82Å well width $Al_{0.35}Ga_{0.65}Sb/GaSb$, also

with a 50Å thin layer of grown-in Si, the other one is a 82Å well width $Al_{0.35}Ga_{0.65}Sb/Al_{0.14}Ga_{0.86}Sb$ without Si dopping. The first quantum-well has exactly the same design with that in the first design, and the operation principle utilizes the natural tendency of the carriers to preferentially populate the lowest band-gap energy. In the as-grown case, the carriers preferentially populate the lower band-gap well, resulting in laser operation of 1.55μm wavelength. The second quantum-well in this design has transition energy of 0.951meV which gives out light of 1.3μm wavelength. We are aiming to remove the longer wavelength quantum-well completely, so that the shorter wavelength quantum-well will be in operation. In order to remove a quantum-well after it has been grown, intermixing is undertaken. The fabrication is similar to the previous design, a SiN_x is capped on the surface, and a strip is cut open. The samples are then annealled for a longer period of time, so that the longer wavelength quantum-well is now removed, while the shorter wavelength quantum-well remains unchange. Now the shorter wavelength quantum-well becomes the smallest band-gap energy in the active region, giving out lights at 1.3μm(capped) and 1.55μm(uncapped) wavelength. In Figure 2, we present the transition energy of both quantum-wells under the effect of annealling.

The optical gain of the two laser diode structure is plotted in Figure 3. The optical gain for the shorter wavelength quantum-well structure in both designs have the same magnitude, since both of them are basically the same structure. It is more interesting to focus on the 1.3μm wavelength emission between the two different designs. The second design shows a higher optical gain in magnitude compared to the first one. The reason for the lower values in optical gain for the first design is that the optical confinement after such a long diffusion length is not as good as the square quantum-well for the same emission wavelength. Hence, the threshold current for 1.3μm wavelength emission in the second structure is lower than that in the first structure. Another advantage of second design over the first one is about the annealling time. It is necessary for the first design to control the annealling time accurately, since time does control the emission of the second wavelength. The second design however, allows a longer diffusion time, so that the quantum-well can be removed completely.

4. Conclusion

This paper has presented a study of two laser diode designs, both of them have the advantage that they does not need a regrowth on the active layer, and both of them utilize intermixing for the control of the 1.3μm wavelength. Both of the designs are dual-strip design, where emission wavelengths are 1.3μm and 1.55μm. However, the first design, which control the annealling time for the second wavelength, requires an accurate annealling time control, and its optical gain is lower compared to the second design. The second design, by growing an asymmetry quantum-well, is capable of emitting 1.55μm and 1.3μm wavelengths, but the 1.55μm quantum-well is removed by intermixing. This design does show to provide a higher optical gain, and the control of annealling time is not as important as the first one.

5. Acknowledgments

This work was supported in part by the RGC earmarked grant of Hong Kong, The University of Hong Kong CRCG research grant and the DAAD-RGC grant between Hong Kong and Germany.

6. References

1. S. Sakai, T.Aoki, and M. Umeno, *Electron. Lett.* **18**, 17 (1982).
2. S. Sakai, T.Aoki, and M. Umeno, *Electron. Lett.* **18**, 18 (1982).
3. J.S. Major, Hun., D. F. Welch, W. E. Plano, and D. Scifres, *Electron. Lett.* **28**, 391 (1992).
4. H. Nagai, Y. Suzuki, and Y. Noguchi, *Electron Lett.* **18**, 371 (1982).
5. N. Bouadma, J. C. Bouley, and J. Riou, *Electron lett.* **18**, 871 (1982).
6. A. B. Piccirilli, N. K. Dutta, L. A. Greuzka, R. F. Karlicek, and J. D. Wynn, *Electron Lett.* **24**, 1565 (1988).
7. K. J. Beernink, R. L. Thornton, and H. F. Chung, *Appl. Phys. Lett.* **64**, 9 (1994).
8. K. J. Beernink, D. Sun, R. L. Thornton and D. W. Treat, *Appl. Phys. Lett.* **68**, 3 (1996).
9. T. E. Schlesinger and T. Kuech, *Appl. Phys. Lett.* **49**, 9 (1986)
10. M. Abramowitz and I. A. Stegun, Handbook of Mathematical Functions (1964).
11. J. M. Luttinger and W. Kohn, *Phys. Rev.* **97**, p.869 (1955).
12. D. J. Ben-Daniel and C. B. Duke, *Phys. Rev.* **152**, p.638 (1966).
13. U. Ekenberg, *Phys. Rev. B.* **40**, p.7714 (1989).
14. K. S. Chan, *J. phys. C.* **19**, p.L125, (1986).

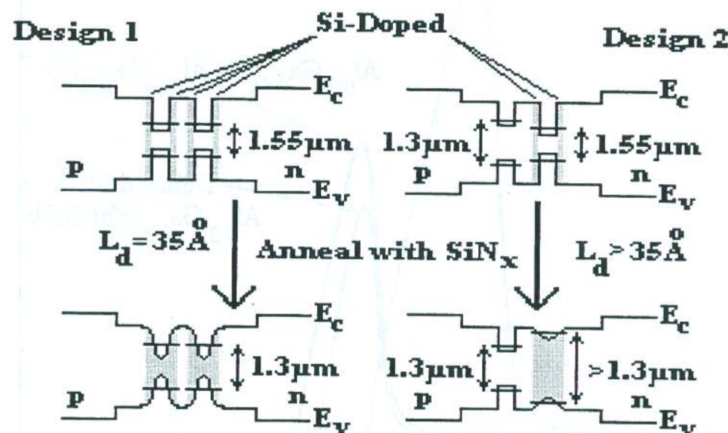

Figure 1. Schematic diagram of the active region of the two designs under the effect of intermixing. The above diagram represents the region where SiN_x cap is cut open, the below diagram represents the region where SiN_x cap is on.

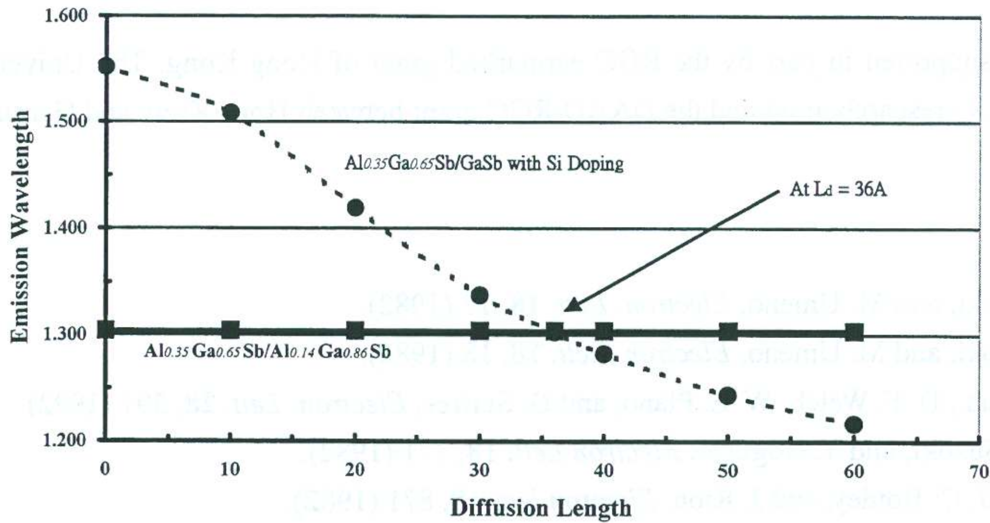

Figure 2. The quantum-well emission wavelength as annealling time increases. Dotted line represents the $Al_{0.35}Ga_{0.65}Sb/GaSb$ quantum-well with Si doping and SiN_x cap on. Solid line represents the $Al_{0.35}Ga_{0.65}Sb/Al_{0.14}Ga_{0.86}Sb$ quantum-well without Si doping and cap opens.

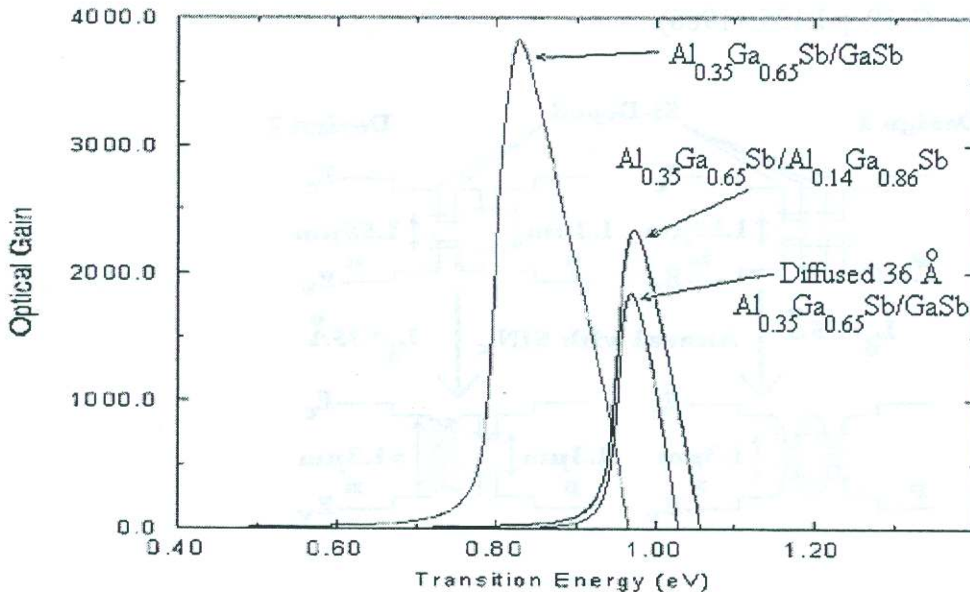

Figure 3. The optical gain of 1.55μm wavelength emision is same for both design, while second design shows a better optical gain than the first design at 1.3μm wavelength.